Letter

Surface Review and Letters, Vol. 7, Nos. & 2 (2000) 7–14

EPITAXIAL GROWTH OF SiO_2 ON Mo(112)

T. SCHROEDER, M. ADELT, B. RICHTER, M. NASCHITZKI,
M. BÄUMER* and H.-J. FREUND
Fritz-Haber-Institut der Max-Planck-Gesellschaft,
Faradayweg 4–6, 14195 Berlin, Germany

Received 3 September 1999

A new preparation is reported which, for the first time, results in a thin, crystalline SiO_2 film on a Mo(112) single crystal. The procedure consists of repeated cycles of silicon deposition and subsequent oxidation, followed by a final annealing procedure. AES and XPS have been used to control film stoichiometry. LEED pictures of high contrast show a hexagonal, crystalline SiO_2 overlayer with a commensurate relationship to the Mo(112) substrate. The wetting of the substrate by the film has been investigated by LEED, XPS and TDS, revealing that the film covers the substrate completely.

1. Introduction

The interest in preparing and investigating thin SiO_2 films originates from various technological fields, such as semiconductor technology or heterogeneous catalysis.

In the semiconductor industry, for example, the properties of thermally grown, amorphous SiO_2 and the Si–SiO_2 interface are decisive for the performance of many electronic devices.[1–3] New generations of high density random access memories (RAM's) and electrically erasable read-only memories (E^2ROM's) as well as metal oxide semiconductor field effect transistors (MOSFET's) require a drastic reduction of the thickness of the insulating SiO_2 layer. In this connection, a complete understanding of the properties of thin SiO_2 layers on Si as well as on new materials, such as SiC,[4] is essential.

Another field where SiO_2 plays a central role is heterogeneous catalysis. Here, it is often used as a support material for highly dispersed metal catalysts. Thin SiO_2 films can thus be used as model supports in studies aiming at a fundamental understanding of the properties of such systems. This approach offers the advantage that all surface science techniques relying on good electrical and thermal conductivity of the samples can be utilized without any restrictions (e.g. charging problems).[5–9] This strategy has, for instance, been successfully applied in the case of a thin, well-ordered Al_2O_3 film grown on a NiAl(110) single crystal.[10] Thin well-ordered SiO_2 films, however, have not been available up to now, as all techniques reported so far (oxidation of Si, deposition of Si on refractory metals) resulted in stoichiometric but amorphous films.[11,12] For the first time,† we report a procedure for the growth of a thin crystalline SiO_2 film on a Mo(112) single crystal.

2. Experimental

The cleaning of the Mo(112) surface is performed as described in the literature,[13] i.e. by oxidation at 1500 K and subsequent heating to 2300 K. Reference spectra taken immediately after crystal cleaning are labeled with the number 0 in the following.

The film preparation starts with four cycles of silicon deposition, each followed by an oxidation step. During the Si deposition, approximately half a monolayer of Si is evaporated by electron bombardment of a silicon rod while the crystal is kept at 300 K.

*Corresponding author. Fax: ++49-30-84134312. E-mail: bacumer@fhi-berlin.mpg.de
†After submission of the article, we have come to know that also in the group of Y. Murata (Physics Department, The University of Electro-Communications, Chofu, Tokyo 182-8585, Japan) well-ordered silicon dioxide films have been prepared on Ni(111).

The subsequent oxidation is carried out at 800 K in an atmosphere of about 5×10^{-5} mbar O_2 for 6 min.[11] During SiO_2 film deposition, spectra have been taken after each oxidation step and are denoted according to the corresponding cycle (1–4). After the deposition, four annealing steps have been applied to order the film. For this purpose, the crystal is heated in an oxygen atmosphere of 5×10^{-6} mbar to 1000 K (first two annealing steps) and 1150 K (last two annealing steps) for 20 min. Spectra taken during SiO_2 film annealing are denoted by the numbers 5–8 according to the respective annealing step.

The experiments were conducted in two different ultrahigh vacuum chambers. The first setup consisted of a chamber equipped with a four-grid LEED (low-energy electron diffraction) optics, also used for Auger spectroscopy (AES), a differentially pumped quadrupole mass spectrometer for TDS (thermal desorption spectroscopy) and all instruments for the preparation of the sample (gas doser, silicon evaporator). All TD spectra shown here have been obtained after exposing the crystal at 200 K to 20 L deuterium (D_2) (heating rate: $\sim$ 0.5 K/s). The X-ray photoelectron spectra (XPS) were recorded in another chamber utilizing a hemispherical electron energy analyzer (Scienta SES-200) in the constant pass energy mode and non-monochromized Mg K_α radiation. The XPS binding energies reported in the following are referred to the Fermi level of the Mo substrate. The takeoff angle ϕ was 0° with respect to the surface normal for all spectra shown here.

3. Results and Discussion

The Mo(112) surface used for the epitaxial growth of the thin SiO_2 film consists of close-packed atomic rows oriented along $[\bar{1}\bar{1}1]$ which are separated by furrows along the $[\bar{1}10]$ direction.[14] Owing to this furrowed surface, the surface potential is highly anisotropic, resulting in a smooth potential variation along the atomic rows in the $[\bar{1}\bar{1}1]$ direction and a rough potential variation perpendicular to the atomic rows in the $[\bar{1}10]$ direction.

Figure 1 shows the result of our LEED study in terms of the reference surface (0_A and 0_B) and the patterns obtained during SiO_2 film deposition (1–4) and SiO_2 film annealing (6 and 8).

The clean Mo(112) surface (0_A) exhibits a $p(1\times1)$ pattern, irrespective of temperature, indicating that the surface preserves the structure expected from the

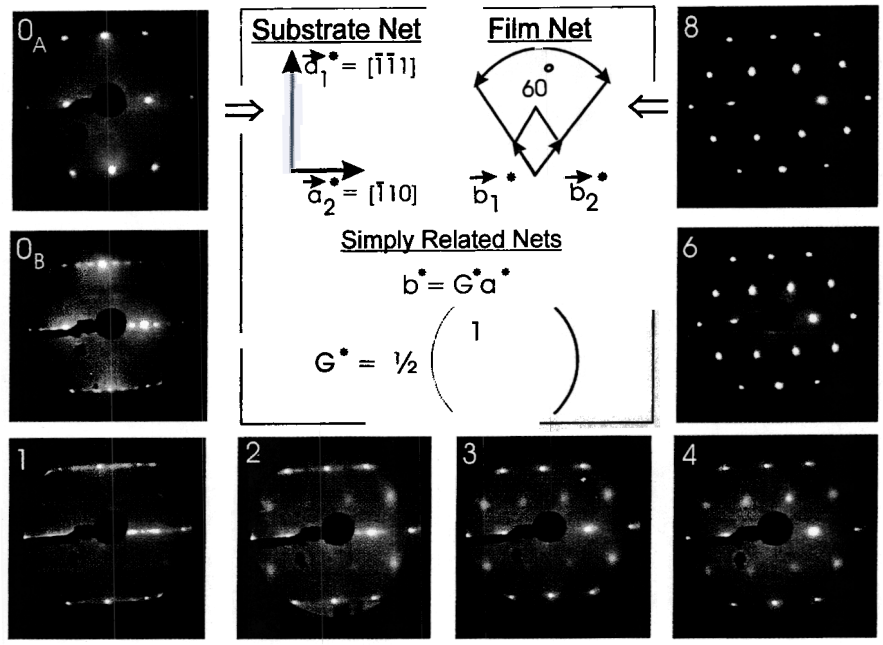

Fig. 1. LEED study ($E = 56$ eV) for the growth of SiO_2 on Mo(112). 0_A — clean Mo(112); 0_B — $p(1\times3)$ pattern of oxygen-modified Mo(112); 1–4 — pictures taken during film deposition; 6,8 — pictures taken during film annealing. Enumeration follows the convention given in the experimental part. The inset shows the substrate and film unit meshes in reciprocal space (above) and the epitaxial relationship (below).

bulk. In the following, the substrate spots will be referred to as fundamental spots. The second important reference surface is a $p(1 \times 3)$ reconstructed surface (0_B) obtained after exposing the clean Mo(112) crystal to oxidation conditions like those applied during film deposition.[15]

After the two first cycles of the film deposition (1 and 2), this $p(1 \times 3)$ superstructure from uncovered substrate regions is still present in the LEED patterns, resulting in a modulated, streaky intensity distribution around the fundamental spots along the $\mathbf{a}_2^*$ direction. Passing from the second (2) to the third cycle (3), however, a pronounced intensity decrease of the $p(1 \times 3)$ pattern is observed which vanishes completely after the fourth cycle (4). This development is accompanied by the appearance of faint and streaky superlattice spots at the center of the rectangular substrate unit mesh (2), showing that the overlayer grows commensurately on the rectangular Mo(112) substrate. These spots gain intensity with progress in film deposition (3 and 4). At the end of the film deposition, the LEED pattern 4 consists of sharp fundamental spots and faint superlattice spots with a relatively high background.

Four annealing steps have been applied (film annealing) to stepwise order the film. Picture 6 shows the situation after two heating steps at 1000 K. The LEED pattern 8 is the final result obtained after two further steps at 1150 K. The superlattice and fundamental spots appear to have similar intensities now and the background intensity is low, confirming the importance of the annealing steps for improving the crystallinity of the film. Taking a hexagonal unit cell as a basis, a value of 5.2 Å can be derived for the length of the unit mesh vector of the film.

Furthermore, it is worth mentioning that the final LEED pattern (8) already provides some interesting information about the defect structure of the film. Whereas all the fundamental spots are sharp and isotropic, the superlattice spots are streaky with an anisotropic broadening along the $[\bar{1}\bar{1}1]$ direction. As described in the literature,[16–18] this points to the formation of antiphase domain boundaries within the overlayer. This also implies that the coverage of the substrate is high or complete. If the film covered only a part of the substrate, i.e. grew in islands, also the fundamental spots should be broadened.[19]

Apart from the structure, the stoichiometry of the film has been studied by means of AES and XPS.

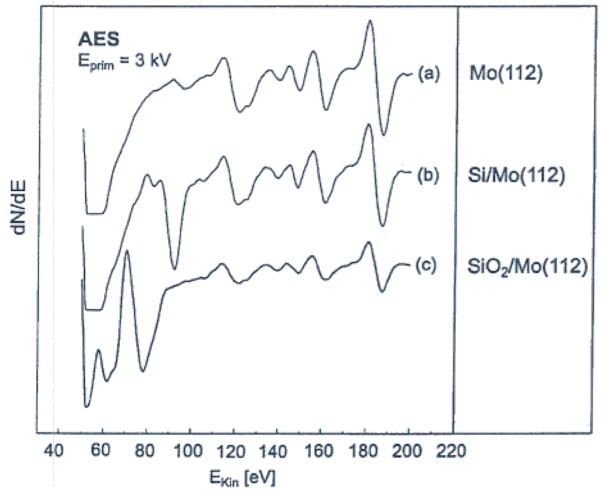

Fig. 2. AES spectra at different stages of film deposition: clean Mo(112) (a), Si deposition on clean Mo(112) (b), SiO_2 film on Mo(112) (c).

Figure 2 shows differentiated Auger electron spectra in the energy range of 50–200 eV taken for the clean Mo substrate (a), after depositing Si (b) and at the end of the film preparation (c). The most intense peak in the Auger spectrum of the clean Mo(112) surface is the $M_{4,5}NV$ transition at 187 eV.[20] The deposition of Si leads to a strong feature at 92 eV in the spectrum which can be assigned to the $L_{2,3}VV$ transition of elemental Si. Due to the high reactivity of Si with respect to oxygen,[21] a small signal is always visible at 84 eV, i.e. close to the position expected for SiO ($L_{2,3}VV$).[22,23] At the end of film preparation, i.e. after the film annealing, the Si $L_{2,3}VV$ line shape is split into a main peak at 78 eV (Si $L_{2,3}V_1V_1$) and a satellite at 64 eV (Si $L_{2,3}V_2V_1$). This spectrum is in line with AE spectra of silica samples,[22,23] thus providing the first evidence of the successful preparation of a stoichiometric SiO_2 film on the Mo substrate. In fact, the presence of SiO can be ruled out by the absence of an Auger transition at 84 eV.[23]

XPS has the advantage that, via the Si_{2p} core level shift, the different Si oxidation states can be resolved.[24] (The position of the elemental Si_{2p} photoelectron line on Mo(112) is found at 99.3 eV.[25]) In Fig. 3, various Si_{2p} photoelectron spectra (left panel) and O_{1s} photoelectron lines (right panel) acquired during SiO_2 film deposition (1–4) and the subsequent SiO_2 film annealing (6 and 8) are presented. The upper insets show the development of position, the lower inset the evolution of intensity.

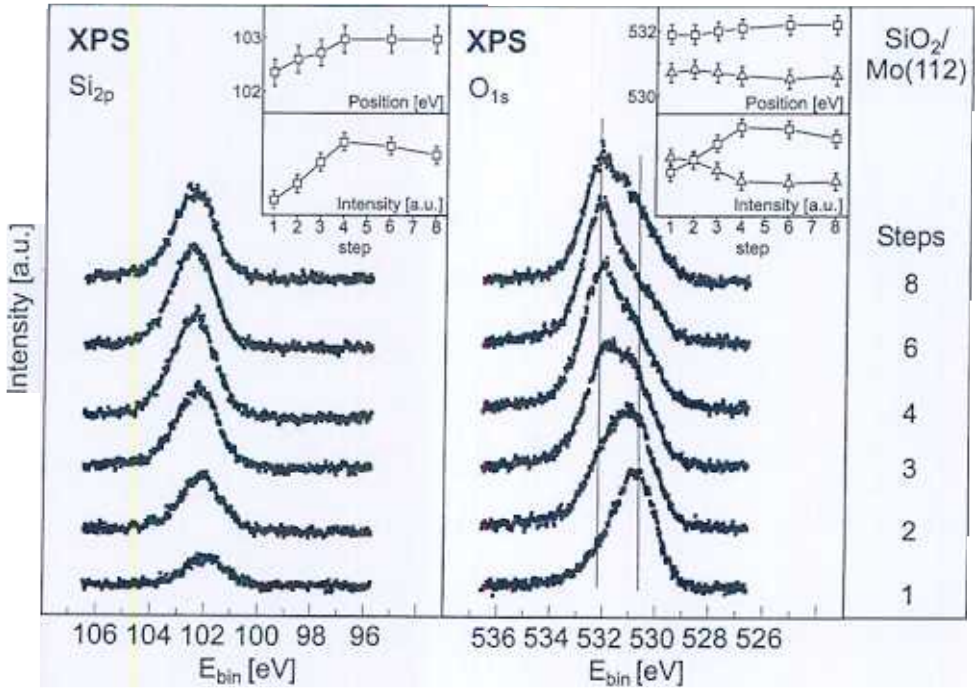

Fig. 3. Si_{2p} (*left panel*) and O_{1s} (*right panel*) photoelectron spectra recorded during SiO_2 film deposition (1–4) and SiO_2 film annealing (6 and 8). The upper insets show the position, the lower inset the intensity of the lines [open squares — Si_{2p} and O_{1s} signal from SiO_2; open triangles — O_{1s} signal from oxygen chemisorbed on Mo(112)].

The first point to note is that the SiO_2/Mo(112) system differs from the SiO_2/Si interface regarding the presence of any silicon suboxides. In the latter case, they are found in a nonstoichiometric transition region of approximately 5 Å to adjust for the inherent density mismatch between SiO_2 and Si. Kuhlenbeck *et al.*[31] succeeded in resolving these suboxides in an investigation of SiO_2 films of less than 10 Å thickness, obtaining chemical shifts of 1.0, 1.8, 2.7 and 3.7 eV for Si^+, Si^{2+}, Si^{3+} and Si^{4+}, respectively. Our XPS study clearly proves the absence of the Si^+ and Si^{2+} state, but, due to the lack of resolution, the Si^{3+} suboxide cannot be resolved from the Si^{4+} state. Since this suboxide is not a stable species, though, it is not likely to be formed at the SiO_2/Mo(112) interface under conditions of oxygen excess.

Regarding the intensities, the nearly linear intensity increase of the Si_{2p} signal during SiO_2 film deposition (1–4) is conspicuous, revealing that the thickness of the film is always much smaller than the inelastic mean free path (IMFP).[26] During SiO_2 film annealing (6 and 8), the Si_{2p} intensity decreases slightly by approximately 15%. Such a silicon loss can be the consequence of SiO_2 evaporation from rough surface regions having a higher vapor pressure[27] or desorption of volatile SiO.[28] The second point concerns the binding energy (BE) of the Si_{2p} signal. During film deposition (1–4), a clear binding energy shift of the Si^{4+} core level can be observed as a function of film thickness (chemical shift increasing from 3.1 eV (102.4 eV) after the first to 3.6 eV (102.9 eV) after the fourth deposition cycle). Note that this shift is merely dependent on the film thickness and not on film order. Film annealing only results in a slight decrease of the FWHM from 1.8 eV to 1.7 eV, but in no change of the Si_{2p} BE (6 and 8). The BE shift of the Si^{4+} core level with film thickness is well known from the SiO_2–Si interface for films up to about 10 Å.[29–31] Here, an explanation based on the dielectric discontinuity across the interface has been proposed[32] and corroborated by a theoretical study of Pasquarello *et al.*[33] This seems to be a reasonable interpretation also in the present case, since other reasons, discussed in the literature, such as charging effects,[34] can be excluded due to the advantageous situation of studying the

film on a metallic substrate. The experimentally observed insensitivity of the Si^{4+} BE with respect to the crystallinity of the film further supports the theoretical work from Pasquarello *et al.*[33] and therefore structural aspects, as proposed by Grunthaner *et al.*, seem unlikely as well.[24]

Next to the Si_{2p} spectra, the corresponding O_{1s} photoelectron spectra can be found in Fig. 3. Apparently, the signal consists of two peaks, one at 530.7 eV resulting from oxygen chemisorbed on Mo(112) (open triangles in the insets)[35] and another one at 532.2 eV (open squares in the insets), which can be attributed to oxygen tetrahedrally coordinated to Si.[24]

The peak at 530.7 eV is the dominating feature after the first and second film deposition cycles (1 and 2) pointing to a submonolayer surface coverage at this stage. As in the LEED study, the most pronounced intensity decrease for chemisorbed oxygen on Mo(112) ($\sim$ 40%) occurs when passing from the second (2) to the third (3) deposition cycle. The fourth deposition cycle (4) results in a further intensity decrease. During the film annealing (6 and 8), however, no detectable change with respect to the intensity or position of the signal is observed. The constant residual intensity as well as the position may be taken as an indication of an interface oxygen species, but could also be due to slight oxygen diffusion into molybdenum.[36]

The intensity of the peak at 532.2 eV increases proportionally to the Si signal with an intensity ratio of approximately 2. As a function of film thickness, no binding energy shift of this photoelectron line is observable within the accuracy of the fitting procedure. The film annealing does not change the position either, but a loss of oxygen bound to silicon (in analogy to the Si_{2p} signal!) and a slight decrease in the FWHM of about 0.1 eV from 1.9 eV to 1.8 eV can be detected. The energy separation between the Si_{2p} and the O_{1s} signal amounts to 429.3 ± 0.4 eV, which, according to Grunthaner *et al.*,[24] is related to the Si oxidation state. Whereas all the suboxides Si_2O, SiO and Si_2O_3 show $\Delta E[O_{1s} - Si_{2p}]$ values higher than 432 eV, only SiO_2 results in an energy difference of 429.5 eV.

In order to study the influence of the film preparation on the Mo substrate, Mo_{3d} spectra have been taken which are presented in Fig. 4. A first set of spectra has been recorded during the different stages of the film preparation and, for reference, a

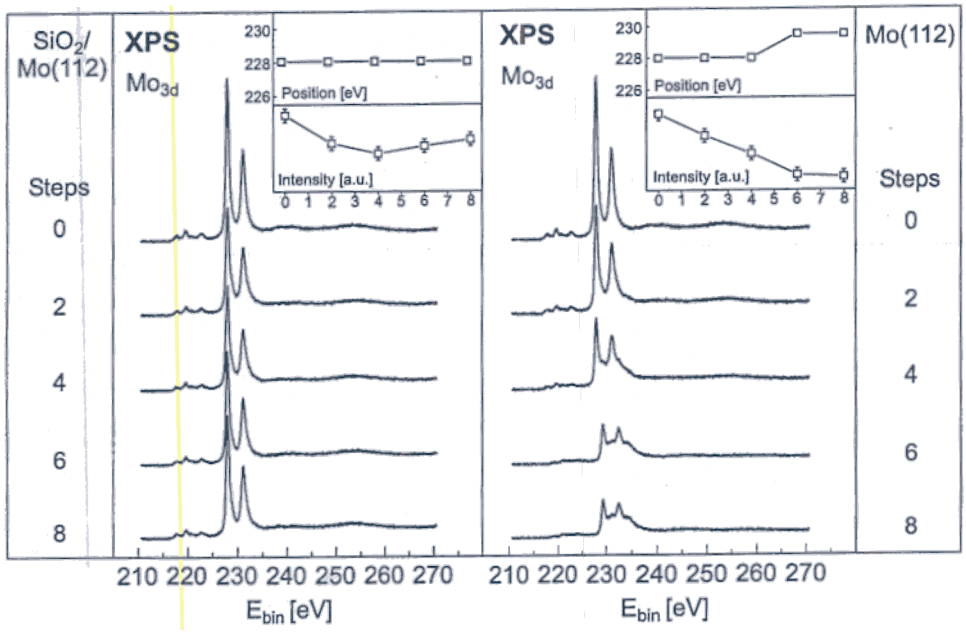

Fig. 4. Behavior of the Mo_{3d} photoelectron line under film preparation conditions with a growing SiO_2 film (*left panel*) and without a growing SiO_2 film (*right panel*). The upper and lower insets show the intensity and position of the line, respectively.

second set without depositing any Si. This allows to compare the behavior of the molybdenum substrate under the preparation conditions with and without film growth.

In the first case, the molybdenum signal is attenuated during film deposition (left panel of Fig. 4, steps 2 and 4), but regains intensity ($\sim$ 15%) during film annealing (steps 6 and 8). This is consistent with the observed Si loss (see Fig. 3). It is noteworthy that no shift in the binding energy of the Mo_{3d} line position can be detected throughout the whole procedure. Consequently, any oxidation of the molybdenum or compound formation between Mo and Si can be excluded.[11,35]

In the second case (see right panel of Fig. 4), a strong intensity attenuation of the Mo_{3d} line can be observed as well, if the film deposition conditions (2 and 4) are applied. During the annealing steps (6 and 8), the signal decreases further and finally reaches a saturation value. Although the shape and BE of the Mo_{3d} line do not alter during the first part of the preparation (2 and 4), the appearance of the spectrum changes drastically when applying the film annealing conditions (6 and 8). In fact, a fit procedure reveals that each spin–orbit component is now split into two components with an intensity ratio of approximately 1 : 2. According to the literature, such a spectrum is characteristic for MoO_2.[37] The new line positions for the more (less) intense spin–orbit components are 229.4 eV (231 eV) for Mo $3d_{5/2}$ and 232 eV (234.2 eV) for Mo $3d_{3/2}$, resulting in a shift of 1.6 eV (3.1 eV) with respect to the metallic state. Since uncovered substrate regions are obviously completely oxidized to MoO_2 under the film annealing conditions, the film coverage θ can be estimated by evaluating possible contributions of the MoO_2 spectrum to the spectrum of the SiO_2/Mo(112) system. By a peak fit procedure, using the line positions and intensity distributions found for MoO_2 as input parameters, an overlayer coverage of at least 95% can be calculated.

In order to tackle the question of coverage in more detail, a TDS experiment has been carried out. As a probe molecule D_2 has been chosen, because it does not adsorb on SiO_2 above 100 K.[38] In Fig. 5, a set of TD spectra collected during the different stages of the film preparation is presented. The clean Mo(112) surface (0) shows two, clearly distinguishable adsorption features at 300 K and 395 K and a shoulder at

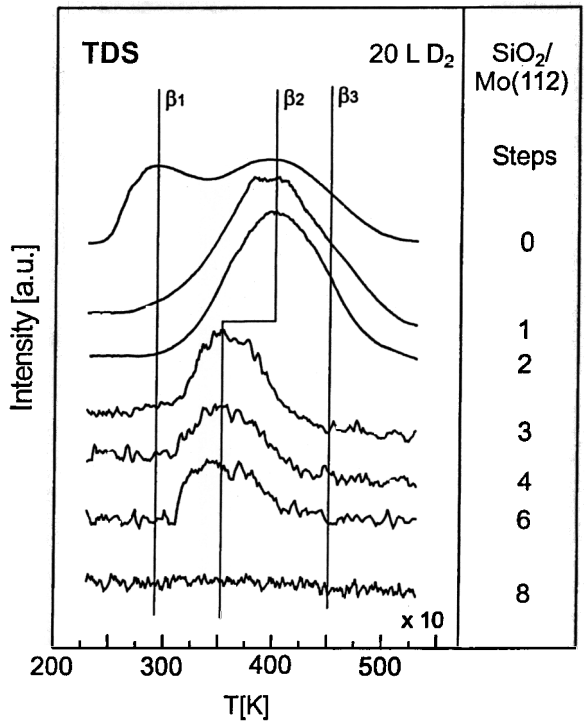

Fig. 5. Set of D_2 TD spectra for a dosage of 20 L D_2 at a substrate temperature of 200 K taken during film deposition (1–4) and film annealing (6 and 8).

about 450 K. These desorption states are referred to as the β_1-, β_2- and β_3- states in the literature.[39,40] The first deposition cycle results in the disappearance of the β_1- state, but leaves the other two states nearly unaffected (1). Whereas the second deposition cycle (2) only results in a slight decrease of the β_3- state (450 K), the most pronounced intensity decrease takes place when passing from the second (2) to the third deposition cycle (3). This decrease is accompanied by a shift to a lower desorption temperature (350 K). The first two film annealing steps (6, 1000 K) do not involve significant changes in the spectrum. Applying the annealing steps to 1150 K (8), however, a complete blockage of D_2 adsorption is achieved.

The interpretation of the TDS data is complicated by the fact that the Mo(112) surface does not remain inert, but is modified by the oxygen exposure under the film preparation conditions. Poisoning of surfaces by electronegative adsorbates is a well-established phenomenon in catalysis and can strongly influence D_2 adsorption.[41,15] As discussed, an ordered $p(1 \times 3)$ overlayer of chemisorbed oxygen

on the Mo substrate is initially formed under film deposition conditions (see Figs. 1 and 3). Clearly, this phase shows a significant D_2 uptake, as confirmed by spectra 1 and 2 in Fig. 5. At this stage, the coverage θ is in the submonolayer region. From the drastic decrease of D_2 adsorption after the third cycle it can be concluded that the monolayer is closed here. This is in line with the LEED and XPS results. Under the film annealing conditions, uncovered areas should be oxidized to MoO_2 (see XPS). In this context, it is important to know that MoO_2 adsorbs D_2 as well.[42] Therefore, the complete blockage of D_2 adsorption signals can indeed be attributed to the growth of a two-dimensional, continuous SiO_2 film on the Mo(112) support.

The thickness of the final film has been estimated in two different ways. On the one hand, the damping of the Mo Auger signal has been used. Assuming an exponential decay of the substrate intensity with an inelastic mean free path (IMFP) of $\lambda_{Mo}^{SiO_2} = 13$ Å,[43] a thickness of about 5–8 Å is calculated. On the other hand, angle-resolved XPS has been applied. Here, the thickness can be obtained by measuring the ratio of the film signal and substrate signal for various takeoff angles ϕ (against the surface normal).[44] In the present case, data for takeoff angles ϕ ranging from 0° to 60° have been collected. The determined values for the film thickness range between 5 and 8 Å and thus agree perfectly with the AES data.

4. Conclusion

XPS and AES prove the successful preparation of a stoichiometric SiO_2 film free of any suboxides on a Mo(112) substrate. For the first time, LEED pictures of a growing SiO_2 film have been obtained showing that the SiO_2 film grows commensurately on the rectangular Mo(112) surface. The quality of the LEED pattern points to a high degree of crystallinity within the overlayer. The growing film protects the underlying Mo(112) from oxidation during the preparation. This and the suppression of any deuterium adsorption (TDS) provide strong evidence for the formation of a two-dimensional, continuous SiO_2 film. The film thickness is determined via AES and ARXPS and ranges for the different, well-ordered films between 5 and 8 Å. This agrees well with the unit cell height of typical SiO_2 low pressure modifications. Since the unit cells of the different SiO_2 modifications are complex and differ only slightly, the epitaxially grown SiO_2 film on Mo(112) has not yet been consistently assigned to a particular SiO_2 phase, but a dynamical LEED study is under way to answer this question.

References

1. S. T. Pantelides, *The Physics of Silicon Dioxide and Its Interfaces* (Pergamon, 1978).
2. C. Helms and B. Deal, *The Physics and Chemistry of Silicon Dioxide and the Silicon/Silicon Dioxide Interface* (Plenum, New York, 1988).
3. C. Helms and B. Deal, *The Physics and Chemistry of Silicon Dioxide and the Silicon/Silicon Dioxide Interface* (Plenum, New York, 1993).
4. J. Bernhardt, J. Schardt, U. Starke and K. Heinz, *Appl. Phys. Lett.* **74**, 1084 (1999).
5. M. Bäumer and H.-J. Freund, *Prog. Surf. Sci.* **61**, 127 (1999).
6. C. Campbell, *Surf. Sci. Rep.* **27**, 1 (1997).
7. C. Henry, *Surf. Sci. Rep.* **31**, 231 (1998).
8. D. W. Goodman, *Surf. Rev. Lett.* **2**, 9 (1995).
9. D. W. Goodman, *Surf. Sci.* **299/300**, 837 (1994).
10. R. Jaeger *et al.*, *Surf. Sci.* **259**, 235 (1991).
11. X. Xu and D. Goodman, *Surf. Sci.* **282**, 323 (1993).
12. J. Mayer, R. Lin and E. Garfunkel, *Surf. Sci.* **265**, 102 (1992).
13. R. G. Musket, W. McLean, C. D. and W. J. Siekhaus, *Appl. Surf. Sci.* **10**, 143 (1982).
14. O. Braun and V. Medvedev, *Sov. Phys. Usp.* **32**, 328 (1989).
15. K. Fukui, T. Aruga and Y. Iwasawa, *Surf. Sci.* **281**, 241 (1993).
16. A. Wilson, *X-Ray Optics* (Methuen, London, 1962) 2nd edition.
17. J. Libuda, F. Winkelmann, M. Bäumer, H.-J. Freund, Th. Bertrams, H. Neddermeyer and K. Mueller, *Surf. Sci.* **318**, 61 (1994).
18. J. Wollschlger, J. Falta and M. Henzler, *Appl. Phys.* **A50**, 57 (1990).
19. J. Tracy and J. Blakely, in *The Structure and Chemistry of Solid Surfaces*, ed. G. Somorjai (Wiley, New York, 1969).
20. C. Zhang, M. H. and G. A. Somorjai, *Surf. Sci.* **149**, 326 (1984).
21. A. Hiraki, *Surf. Sci. Rep.* **3**, 357 (1984).
22. B. Carriere and B. Lang, *Surf. Sci.* **64**, 209 (1977).
23. B. Carriere and J. P. Deville, *Surf. Sci.* **80**, 278 (1979).
24. F. J. Grunthaner, P. J. Grunthaner, R. Vasquez, B. Lewis, J. Maserjian and A. Madhukar, *J. Vac. Sci. Technol.* **16**(5), 1443 (1979).
25. J. Moulder, W. Stickle, P. Sobol and K. Bomben, *Handbook of X-Ray Photoelectron Spectroscopy* (Perkin-Elmer, 1992).

26. D. F. Mitchell, K. B. Clark, J. A. Bardwell, W. N. Lennard, G. R. Massoumi and I. V. Mitchell, *Surf. Interf. Anal.* **21**, 44 (1994).
27. I. Markov, *Crystal Growth for Beginners* (World Scientific, 1995).
28. R. Walkup and S. Raider, *Appl. Phys. Lett.* **53**, 888 (1988).
29. Z. Lu, M. Graham, D. Jiang and K. Tan, *Appl. Phys. Lett.* **63**(21), 2941 (1993).
30. G. Hollinger and F. Himpsel, *Appl. Phys. Lett.* **44**(1), 93 (1984).
31. W. Braun and H. Kuhlenbeck, *Surf. Sci.* **180**, 279 (1987).
32. R. Browning, M. Sobolewski and C. Helms, *Phys. Rev.* **B38**, 13407 (1988).
33. A. Pasquarello, M. Hybertsen and R. Car, *Phys. Rev.* **B53**, 10942 (1996).
34. Y. Tao, Z. Lu, M. Graham and S. Tay, *J. Vac. Sci. Technol.* **B12**(4), 2500 (1994).
35. J.-W. He, X. Xu, J. Corneille and D. Goodman, *Surf. Sci.* **279**, 119 (1992).
36. F. P. Wang, P. Wang, K. Lu, Z. Fang, M. Gao, X. Duan, M. Cui, H. Ma and X. Jiang, *J. Appl. Phys.* **85**, 3175 (1999).
37. B. Brox and I. Olefjord, *Surf. Interf. Anal.* **13**, 3 (1988).
38. C. Ko and R. Gorte, *Surf. Sci.* **155**, 296 (1985).
39. G. Lopinski, J. Prybyla and P. Estrup, *Surf. Sci.* **296**, 9 (1993).
40. G. Lopinski, J. Prybyla and P. Estrup, *Surf. Sci.* **315**, 269 (1994).
41. M. Kiskinova, *Surf. Sci. Rep.* **8**, 359 (1988).
42. A. Katrib, V. Logie, N. Saurel, P. Wehrer, L. Hilaire and G. Maire, *Surf. Sci.* **377–379**, 754 (1997).
43. M. Seah and W. Dench, *Surf. Interf. Anal.* **1**, 2 (1979).
44. C. Fadley, *Prog. Surf. Sci.* **16**, 275 (1984).